IEEE Access
Multidisciplinary | Rapid Review | Open Access Journal

Received 19 September 2025, accepted 13 October 2025, date of publication 20 October 2025, date of current version 24 October 2025.

Digital Object Identifier 10.1109/ACCESS.2025.3623242

RESEARCH ARTICLE

Performance Evaluation of Bluetooth Channel Sounding on Commercial Hardware

JORG WIEME[1], RUBEN NIETVELT[2], (Graduate Student Member, IEEE), DRIES VAN LEEMPUT[3], MAARTEN WEYN[2], (Senior Member, IEEE), PIETER CROMBEZ[3], (Member, IEEE), RAFAEL BERKVENS[2], (Member, IEEE), ELI DE POORTER[1], AND JEROEN HOEBEKE[1]

[1]Department of Information Technology, imec - IDLab, Ghent University, 9000 Ghent, Belgium
[2]Faculty of Applied Engineering, imec - IDLab, University of Antwerp, 2000 Antwerp, Belgium
[3]Televic Healthcare, 8870 Izegem, Belgium

Corresponding author: Jorg Wieme (jorg.wieme@ugent.be)

This work was supported in part by the DistriMuSe project through HORIZON-KDT-JU-2023-2-RIA under Grant 101139769, and in part by the imec.icon Project UBIWAU, funded by imec and Flanders Innovation & Entrepreneurship.

ABSTRACT This paper presents a performance evaluation of Bluetooth Channel Sounding, a feature introduced in Bluetooth 6.0, tested on commercially available hardware. The evaluation includes a publicly accessible dataset containing raw Channel Sounding measurements annotated with millimeter-accurate ground truth, and metadata of the measurement campaign. Results demonstrate that Channel Sounding is well-suited for its primary envisioned use case, which is secure proximity detection in keyless entry systems. Its accuracy at close range ensures reliable unlocking when the user is truly nearby, while errors at longer distances are less critical, as access would not be granted regardless. Moreover, it also shows promise for indoor localization, offering encouraging initial results for future deployment of localization with Channel Sounding. However, the presence of outliers can significantly affect accuracy and must be accounted for in practical applications. The evaluation underscores the impact of algorithm choice, configuration parameters, and environmental conditions on performance. While the approach is promising, single-antenna setups currently lack the robustness needed for high-precision localization, highlighting the need for more accurate algorithms and system-level improvements. The dataset and analysis provide a foundation for future improvements through advanced signal processing and machine learning techniques.

INDEX TERMS Bluetooth channel sounding, bluetooth HADM, bluetooth low energy, dataset, distance estimation, PBR.

I. INTRODUCTION

Accurate indoor localization has become a critical capability in modern wireless systems [1], driven by the growing demand for context-aware services in environments where satellite-based positioning systems like Global Positioning System (GPS) are ineffective. GPS signals, which rely on Line-Of-Sight (LOS) communication with satellites, are significantly attenuated or completely blocked by walls and other structural elements [2], making them unreliable or unusable indoors. However, many industries rely heavily on indoor localization to enhance their operations and services. In healthcare, it allows real-time patient tracking [3], improves emergency response times, and supports efficient allocation of medical equipment. In industrial environments, it facilitates precise asset tracking [4], improves workflow automation, and can improve worker safety.

To meet these needs, various wireless technologies have developed their own approaches to indoor localization. Solutions based on Ultra Wideband (UWB) [5], [6], [7], Wi-Fi [8], Zigbee [9] and Bluetooth, each offering unique advantages and limitations in terms of accuracy, infrastructure requirements, power consumption, and device compatibility.

The associate editor coordinating the review of this manuscript and approving it for publication was Cesar Vargas-Rosales.

Bluetooth, originally introduced to replace wired serial communication, has evolved significantly over the years. With the introduction of Bluetooth Low Energy (BLE) in version 4.0 [10], the technology became a key enabler for the growing Internet of Things (IoT). The first step of Bluetooth-based ranging was the use of Received Signal Strength Indicator (RSSI), which provided only rough estimates [11], [12], [13]. RSSI-based ranging is simple and widely supported, but it suffers from high variability making it unreliable for precise distance estimation. Later versions, particularly 5.1 [14], introduced features aimed at improving location awareness. This was released under the name of Direction Finding (DF) [15], which uses antenna arrays to estimate the Angle of Arrival (AoA) or Angle of Departure (AoD) of a signal. While this method offers better accuracy [16], it requires multiple antennas and careful calibration. This increases the complexity and cost of devices, making it less suitable for compact or low-power applications.

To address these limitations, Bluetooth 6.0 [17] introduced Channel Sounding (CS) [18], also referred to as High Accuracy Distance Measurement (HADM). CS has the potential to outperform previous Bluetooth-based ranging methods. Although the specification defines CS execution at the controller level, it leaves data interpretation and performance to the developers' choice. This flexibility allows for a broad range of implementation strategies, each with its own trade-offs.

This paper presents a performance evaluation of Bluetooth Channel Sounding using commercial hardware in various settings. The contributions are as follows:

- Conduct an initial assessment of how different algorithmic approaches affect ranging accuracy.
- Evaluate how various environmental conditions influence system performance.
- Examine the impact of device orientation and positioning on performance metrics.
- Analyze how Bluetooth Channel Sounding parameters affect ranging accuracy.
- A publicly available dataset is introduced,[1] containing over 20,000 raw CS measurements labeled with millimeter-accurate ground truth. The dataset covers a range of settings, including indoor and outdoor environments, variations in device orientation and height, different transmission power levels, selected communication channels, and both line-of-sight and non-line-of-sight conditions.

The paper is structured as follows, Section II reviews related work on Bluetooth-based localization and other wireless ranging technologies. Afterwards a technical background on Bluetooth Channel Sounding and its underlying principles is provided in section III. Section IV describes the experimental setup, including the hardware, software, and measurement configurations. Section V presents and analyzes the results obtained from the test scenarios. Section VI discusses the dataset collected during our experiments, including details on its structure and availability. Finally, Section VII concludes the paper and outlines directions for future work.

[1] https://doi.org/10.5281/zenodo.17347695

II. RELATED WORK

The authors of [19] conducted an early evaluation of BLE RSSI for distance estimation, highlighting the instability of signal strength in real-world indoor environments. Building on those issues, the authors in [20] improved distance estimation in vehicular contexts by modeling RSSI distributions using skewed statistical models. However, these systems are used more frequently in the context of localization. For instance, [21] demonstrated that combining signal propagation models with Kalman filtering can yield submeter accuracy in controlled indoor settings, although performance degrades in complex uncontrolled environments.

While Bluetooth DF is primarily explored in the context of localization, several studies have investigated its potential for accurate ranging distance estimation. In [16], the authors demonstrate that firmware-level enhancements and antenna design can significantly improve distance estimation accuracy, achieving sub-meter precision in controlled environments. Similarly, [22] presents an experimental evaluation using commercial devices, showing that DF can yield a mean ranging error of 22 cm in outdoor settings. However, [23] highlights critical limitations in real-world deployments, including angular inconsistencies and hardware sensitivity, which can degrade ranging performance in dynamic or cluttered environments.

Several non-Bluetooth technologies have explored phase-based ranging, direction finding and other methods to achieve high-precision distance estimation. A sub-GHz narrowband system was implemented and evaluated for automotive applications, demonstrating phase-detection ranging in the 920 MHz band [24]. SpotFi is a well-known system that utilizes commodity Wi-Fi hardware to perform high-resolution AoA by exploiting channel state information and super-resolution algorithms, achieving decimeter-level accuracy in indoor environments [25]. Building on this, newer systems have leveraged Wi-Fi 6 features such as OFDMA and MU-MIMO to improve spatial resolution and robustness in multipath conditions [26].

UWB is widely regarded as the most accurate Radio Frequency (RF)-based technology for short-range distance estimation, offering centimeter-level precision and strong resilience to multipath effects [27], [28]. Its adoption is growing in high-end consumer devices, though power consumption and limited availability in low-cost hardware remain key barriers [29]. Similar to other technologies mentioned earlier, the majority of studies focus primarily on localization applications [5], [6], [7].

Several studies have investigated the theoretical potential of Bluetooth CS and proposed algorithmic frameworks for distance estimation. For example, the authors in [30] present a signal processing pipeline for interpreting CS

data, while [31] explores the feasibility of Bluetooth CS in practical scenarios, focusing on the impact of noise and hardware imperfections, attempting to tackle these with a Parametric Neural Network. Similarly, [32] evaluates the performance of various estimation algorithms using controlled testbed data, and [33] compares Bluetooth CS with other ranging technologies, emphasizing its theoretical advantages for wireless car keys. Preliminary and primarily theoretical investigations into the use of Support Vector Regression (SVR), along with other enhancements such as sparse methods, for distance estimation have been presented in [34]and [35]. While both proposed approaches demonstrate slightly better performance than a standard super-resolution algorithm, the evaluation was conducted using an unspecified, likely in-house developed hardware platform and a non-standardized CS protocol, which limits the reproducibility and generalization of the results.

Another very recent study [36] reports achieving a localization error as low as 0.22 meters for distances under 30 meters, under specific assumptions, using a neural network-based method.

Earlier foundational work by [37] and [38] laid the groundwork for Bluetooth-based ranging and localization, though these studies primarily addressed general techniques or general signal processing strategies. Although these contributions are valuable, most existing literature remains focused on theoretical modeling, algorithm design, or simulation-based validation.

Moreover, there is a growing trend toward the commercialization and patenting of Bluetooth CS as well as CS algorithms [39], [40], [41], [42]. This trend has resulted in a rush in proprietary algorithm development, where companies and researchers compete to secure intellectual property around signal processing techniques and ranging accuracy improvements. However, none of these works have provided extensive real-life experiment evaluations, do not provide any open datasets nor do they discuss how the CS impact ranging accuracy.

III. BLUETOOTH CHANNEL SOUNDING

Similar to conventional Bluetooth and BLE, CS operates within the 2.4 GHz Industrial, Scientific, and Medical (ISM) band. However, whereas BLE utilizes 40 channels with a width of 2 MHz each, CS adopts a refined channelization scheme comprising 80 channels with 1 MHz channel width. To minimize interference with primary BLE operations, the channels overlapping with BLE advertising channels 37, 38, and 39 have been explicitly marked as unusable. Consequently, only 72 out of the 80 defined channels are actively employed for Channel Sounding. The distribution of these usable channels is depicted in Figure 1.

As with other BLE operational modes, such as connection mode, CS employs a frequency hopping mechanism. To accommodate the specific requirements of CS, new Channel Selection Algorithms (CSAs) have been designed and are described in the Bluetooth 6.0 specification [17].

Furthermore, based on insights from the implementation of DF, the Bluetooth 6.0 standard introduces support for multiple antenna configurations to improve ranging robustness and accuracy. The revised channel structure and antenna requirements may render many existing Bluetooth chipsets incompatible with CS. Consequently, it is imperative that hardware implementations conform to the Bluetooth 6.0 standard to ensure full functionality. Although the standard supports multiple antenna configurations, this discussion is restricted to single-antenna systems, as such configurations are commonly imposed by the limitations of commercially available hardware.

A. ROUND-TRIP TIMING AND PHASE-BASED RANGING

CS has two ranging methods: Round-Trip Timing (RTT) and Phase-Based Ranging (PBR). As the name suggests, RTT estimates distance by measuring the time it takes for a message to travel to the receiver and back. This process is illustrated on the left side of Figure 2. These timing measurements can then be used to calculate the distance, based on the speed of light denoted as c, using the following equation:

$$RTT = 2 \times t = (t_4 - t_1) - (t_3 - t_2),$$
$$d = \frac{c \times RTT}{2}.$$

However, RTT was primarily introduced in the standard as an additional security mechanism, serving as a boundary for the maximum allowable distance. Moreover, RTT is characterized by relatively low accuracy; internal evaluations have shown average error exceeding 4 meters at a true distance of just 1 meter. This inaccuracy is primarily attributed to the method's sensitivity to clock drift and processing delays, rendering it less suitable for high-precision ranging applications [18]. Given these limitations, the remainder of this work will not focus on RTT.

Whereas RTT estimates distance based on the time-of-flight of a signal combined with the speed of light, PBR leverages a different physical property of electromagnetic waves: their phase. Specifically, it utilizes the relationship between wavelength and frequency, given by $length = \frac{f}{c}$, to infer distance. However, while the phase of a received signal can be measured, the total number of complete wave cycles n that have occurred between the transmitter and receiver remains unknown.

To address this, PBR exploits the phase offset of the received signal, which can be expressed as:

$$\theta = 2\pi \times (\frac{2 \times d \times f}{c} + n),$$

where d is the distance, f is the frequency, and n is the unknown integer number of full cycles. Although n cannot be measured directly, this ambiguity can be resolved by performing measurements across multiple frequencies. By comparing the phase differences between two frequencies,

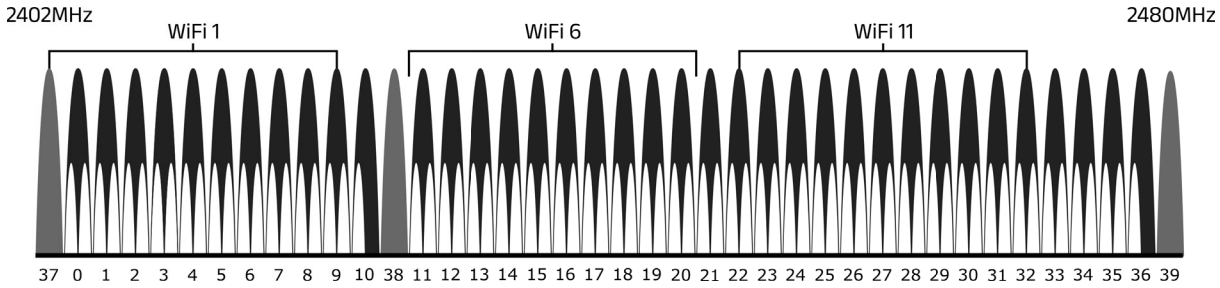

FIGURE 1. Bluetooth Low Energy ISM band spectrum showing both 1 MHz and 2 MHz channel width, and overlapping Wi-Fi channels 1, 6 and 11. Grey channels indicate the primary BLE advertisement channels, black channels represent the secondary data channels, and the new spectrum allocation for Channel Sounding is highlighted in white.

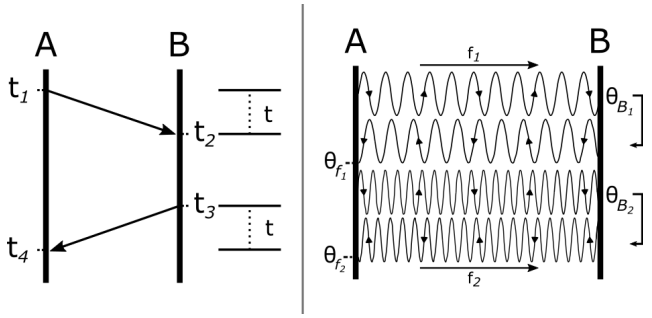

FIGURE 2. Timing diagram of Round-Trip Timing on the left and visualization of the Phase-Based Ranging on the right, where θ_{B_1} and θ_{B_2} represent the phases copied by the receiving node for its transmission.

the distance can be estimated using:

$$d = \frac{c}{4\pi} \times \frac{\theta_{f_2} - \theta_{f_1}}{f_2 - f_1}. \tag{1}$$

The remaining task is to accurately acquire the phase values. As illustrated on the right side of Figure 2, the transmitter records the phase of each transmitted frequency. Upon receiving the signal, the receiver captures its phase and responds using the same frequency and captured phase, effectively reflecting the signal. The original transmitter then receives this reflected signal and measures the round-trip phase offset. This process is repeated at multiple frequencies to improve accuracy. For each frequency pair, a distance estimate is derived from the phase difference. These estimates are then jointly processed using linear regression, which helps resolve phase ambiguities and enhances robustness against noise and multipath effects.

Unlike RTT, PBR does not require clock synchronization between devices, making it more suitable for ranging. However, it introduces potential security vulnerabilities, as demonstrated in [43]. For this reason, Bluetooth CS integrates both RTT and PBR to provide a more robust and secure ranging solution. This integration helps detect relay attacks and similar threats, as such methods typically introduce measurable delays that indicate potential tampering with the PBR process.

B. COMMUNICATION ARCHITECTURE

While RTT and PBR are fundamental concepts applicable to a wide range of wireless technologies, Bluetooth CS introduces additional definitions to ensure structural consistency and interoperability. One of the key elements is the topology: Bluetooth CS operates in a one-to-one configuration, where one device assumes the role of the initiator and the other acts as the reflector. Either device may initiate the ranging process.

Throughout the CS procedure, an Asynchronous Connection-Oriented Logical Transport (ACL) link is maintained between the devices. The initiator may function as either the central or peripheral device in this connection, and the same applies to the reflector. All operations defined by the standard occur at the controller level, while the interpretation and use of data derived from RTT and PBR are left to the discretion of the developer.

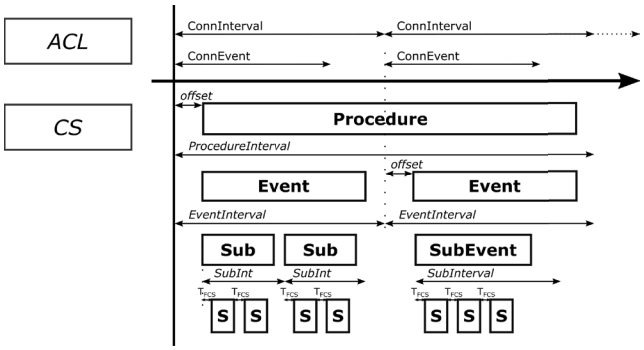

FIGURE 3. Representation of a procedure and its components, illustrating their timing relative to ACL events. At the lowest level of the CS hierarchy, *S* denotes an individual Step, with T_{FCS} indicating the offset between the start of each Step and the beginning of the corresponding Subevent.

The ACL connection must be established prior to initiating CS, and its termination will also end the CS session. During this connection, configuration parameters for CS are exchanged, including the mandatory security settings. As specified in the Bluetooth 6.0 standard [17], the ACL connection must be encrypted to ensure secure communication.

In addition to configuration, the reflector must transmit raw measurement data back to the initiator. This step is currently still essential to address challenges such as accurate phase

reconstruction, compensation for hardware impairments, and robustness against multipath effects and noise. This data transfer can be implemented using proprietary methods or through the standardized Ranging Service [44], which supports both configuration and data exchange.

C. OPERATIONAL LOGIC

Unlike BLE operations, advertising and connection, which are structured around periodic intervals and event-based scheduling, CS introduces a distinct procedural hierarchy. Rather than relying on recurring connection events, CS is organized into a hierarchical time-division structure that ensures precise coordination and interoperability between devices. This structure consists of four nested levels: the CS procedure, CS events, CS subevents, and CS steps. Each level plays a distinct role in the execution of the ranging process and is governed by specific timing rules relative to the underlying ACL connection, displayed in Figure 3.

A CS procedure represents the complete ranging session between two devices. It is always conducted within the context of an active ACL connection. A CS procedure may span multiple connection intervals, allowing extended measurement sessions.

CS events are discrete instances of the CS procedure and are scheduled relative to an ACL connection event. However, the number of CS events does not necessarily correspond to the number of ACL events. Each CS event is initiated at a specific offset from the start of the ACL event, with its timing tightly controlled to ensure synchronization. The controller determines the number of CS events per procedure and their scheduling, allowing flexibility in the frequency of the ranging measurements.

Each CS event comprises one or more CS subevents, which are anchored to the same ACL event as the corresponding CS event. A single CS event may include between 1 and 16 CS subevents. An additional CS subevent interval is defined, ranging from 625µs to 40959.375ms, or 0 if only one subevent is used.

The CS steps constitute the level at which actual RTT and PBR operations occur. Each CS subevent contains at least 2 and up to 160 CS steps. The standard imposes the additional constraint that a single procedure may include no more than 256 CS steps. Each CS step operates in one of four modes: mode-0 is used for calibration, compensating for clock drift that affects frequency generation and timing; mode-1 performs RTT; mode-2 performs PBR; and mode-3 executes a combination of RTT and PBR. Each CS subevent must begin with at least one and up to three mode-0 steps, while the remaining steps may be configured according to the application requirements. The standard also defines a mode sequencing structure to facilitate deterministic scheduling of modes if required by the applications.

Each CS step operates at a distinct frequency, and the CSA is invoked for each step to determine the appropriate frequency. For example, if 50 steps are executed, the CSA is applied 50 times. Although mode-0 may operate on a different PHY, all other modes within a procedure must use the same PHY configuration (1M, 2M, S2 Coded, or S8 Coded).

IV. EXPERIMENTAL SETUP

As defined by the standard and due to its numerous configurable parameters, CS exhibits significant variability. One of its primary intended use cases is wireless car key functionality, offering enhanced security compared to previous Bluetooth-based solutions. However, similar to other ranging technologies, indoor localization is already considered an application, particularly given the potential for higher accuracy than existing Bluetooth-based methods. These two use cases have markedly different requirements. However, localization imposes more stringent constraints, demanding both high accuracy and low latency. Consequently, all experiments in this study were designed with localization performance as the central focus.

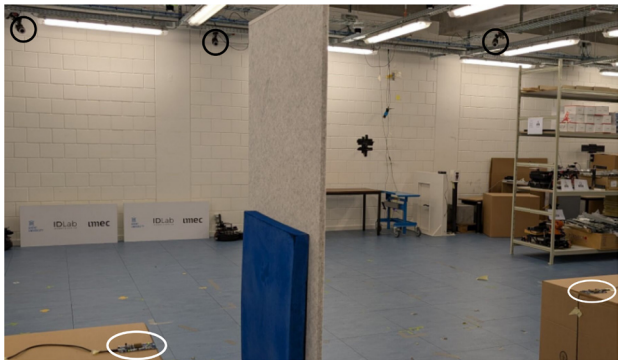

FIGURE 4. Example of a measurement setup in which two devices perform ranging, with an RF absorber positioned 50 centimeters from the initiator. MoCap cameras are indicated in black, while the devices are highlighted in white.

For the PBR steps, while the specification allows for various timing and tone configurations, the mandatory settings defined by the standard were adopted to ensure interoperability, these are also documented in the dataset. Furthermore, to meet the low-latency requirements, the configuration was limited to a single subevent comprising 160 steps, 159 in mode 2 and one in mode 0.

A. HARDWARE AND SOFTWARE

The hardware platform used in this study was the Nordic Semiconductor nRF54L15 DK [45], a development kit featuring the nRF54L15 System-on-Chip (SoC), which is capable of emulating earlier versions of the chip. This SoC is compliant with the Bluetooth 6.0 specification and is among the first commercially available devices to support CS. The development kit includes all necessary peripherals and tools required for both firmware development and experimental evaluation.

For the software stack, version 2.9.1 of the nRF Connect SDK (NCS) [46] was used. NCS is a development framework

built around Zephyr [47], specifically designed for Nordic Semiconductor devices to streamline the development process. Both the Controller and Host components are implemented using Nordic's proprietary stacks. The application layer was based on the Channel Sounding sample provided within NCS [48], which was extended and adapted for the experiments. Data acquisition, algorithmic processing, and analysis were performed using Python, interconnected with the hardware via UART.

FIGURE 5. Example of outdoor measurement setup in which two BLE devices perform ranging.

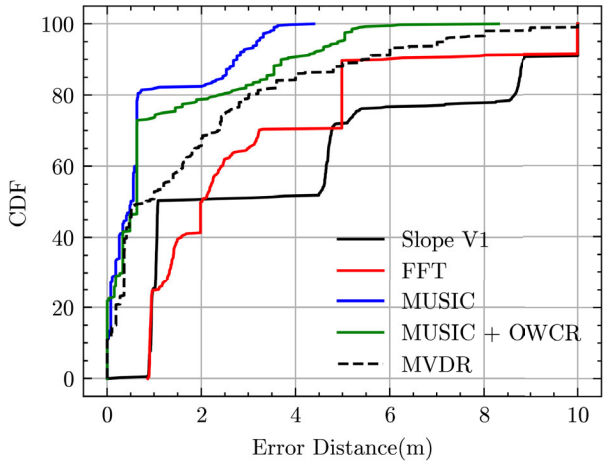

FIGURE 6. Distance errors for a collection of algorithms, evaluated on an indoor LOS dataset spanning a range of distances.

B. MEASUREMENTS SETUP

All indoor experiments were conducted in the Industrial IoT Lab [49], located in Ghent, Belgium. This is an advanced test facility designed to accelerate research and development in production and warehousing IoT technologies. The lab features a $240m^2$ warehouse environment, which includes both open areas and densely packed racks. This setting creates a rich multipath environment with natural interference from coexisting technologies and Bluetooth devices, making it ideal for evaluating the performance of CS. To validate measurement accuracy, a Motion Capture (MoCap) system installed in the warehouse provides millimeter-level ground truth. One of the experimental setups used for data collection is shown in Figure 4. Additionally, a set of measurement locations were conducted outdoors in an open field to capture data in a multipath-free environment, shown in Figure 5. As the MoCap system cannot be deployed in such settings, a measuring wheel was used to estimate distances, although with reduced accuracy due to human error and design.

V. RESULTS AND ANALYSIS

A. ALGORITHMIC INFLUENCE ON PERFORMANCE

Multiple algorithms were analyzed and compared over a distance range of 1 to 10 meters, based on more than 1,000 measurements. Figure 6 presents the distance estimation errors for a selection of algorithms, for indoor LOS. The first is a slope-based algorithm inspired by the Equation 1. A least squares fit is performed on these samples to obtain the final result. The second is an Fast Fourier Transform (FFT)-based approach. For the FFT results, two extreme outliers were excluded due to their disproportionate impact on the distribution. The third and fourth methods are based on Multiple Signal Classification (MUSIC), as proposed in [37], with one implementation using MUSIC alone and the other combining MUSIC with One Way Channel Response (OWCR). MUSIC is an algorithm that relies on several parameters. The parameter settings discussed in [37] and [50] were adopted and adjusted based on observations. Another super-resolution algorithm similar to MUSIC is Minimum Variance Distortionless Response (MVDR), as proposed for Direction Of Arrival (DOA) estimation in [51]. However, the authors themselves acknowledge that it is outperformed by MUSIC, a finding that is also confirmed by the present measurements. The MUSIC-based methods clearly outperform the others in this short-range scenario, achieving accurate results in approximately 80% of the cases. This result, as reported by the authors in [37], is attributed to the narrowband nature and the use of a single-antenna setup.

To assess performance at longer ranges, additional indoor measurement locations were conducted up to 20 meters, leading to an additional 300 measurements across several locations. In this scenario, the slope-based algorithm significantly outperformed the MUSIC-based methods, achieving errors below 2.5 meters in 87% of the cases, whereas MUSIC yielded errors around 8 meters in the same percentile. To further illustrate this, Figure 7 visualizes the MUSIC error as a function of measurement distance. Two factors likely contribute to this performance gap. First, the current MUSIC implementation uses a naive search over a predefined steering vector space, which may limit its adaptability. Second, the algorithm requires an estimate of the number of multipath components, and the metal racks in the warehouse, used for long-range measurements due to space constraints, may act as reflective barriers, complicating multipath prediction,

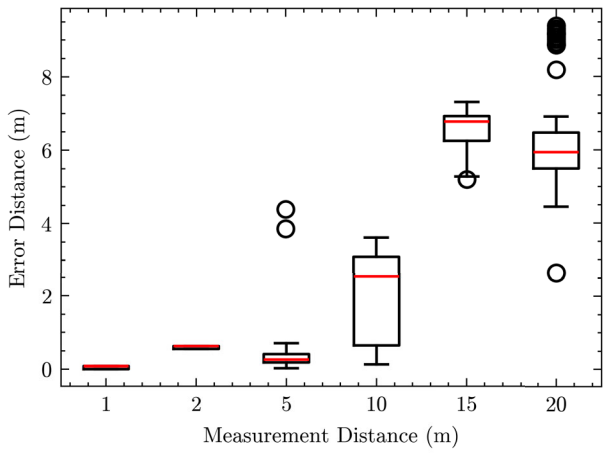

FIGURE 7. Distance estimation errors for MUSIC at various measurement distances, evaluated on an indoor LOS dataset.

or removing them altogether. In contrast, the FFT algorithm showed strong performance in the low-error range, with 40% of the measurements yielding highly accurate results, but also exhibited a similar tail length of poor outcomes.

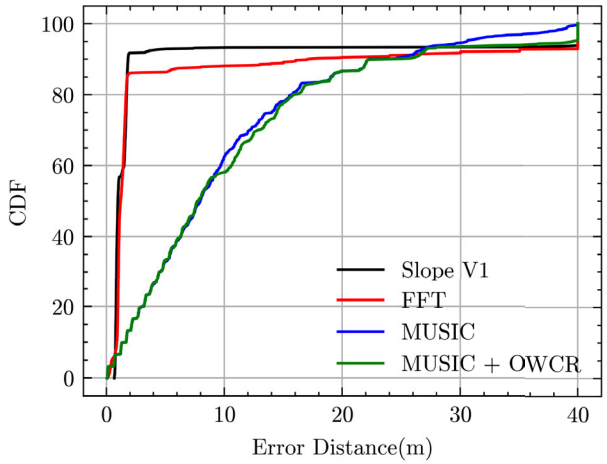

FIGURE 8. Distance errors for various algorithms, evaluated on a LOS outdoor dataset.

Outdoor experiments were also conducted in an open field, covering distances from 1 to 72 meters for LOS and 1 to 20 meters for Non-Line-Of-Sight (NLOS). These results, as illustrated in Figure 8, closely resemble the findings observed in the long-range indoor scenario: the slope-based and FFT algorithms significantly outperformed MUSIC, again likely due to the parameter sensitivity of the latter. In this setting, more than 90% of the more than 800 measurements had errors below 2 meters, with the slope-based method slightly outperforming FFT.

These findings highlight that, while none of the algorithms were fully optimized, they already demonstrate promising performance. The results also underscore the importance of algorithm selection and tuning, particularly in relation to environmental conditions and range requirements.

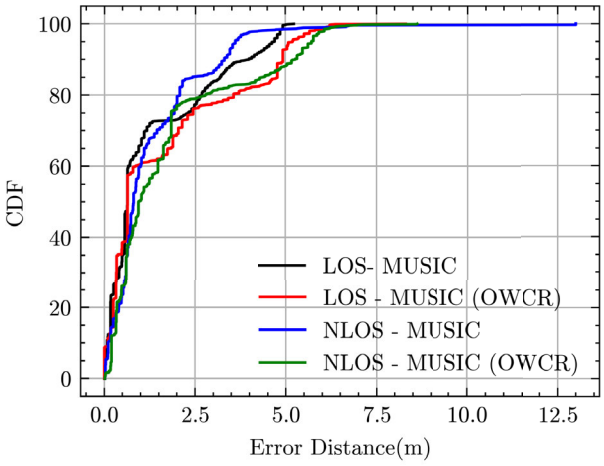

FIGURE 9. Distance errors for MUSIC under both LOS and NLOS conditions, equivalent dataset as the algorithm evaluation.

B. IMPACT OF LINE-OF-SIGHT AND NON-LINE-OF-SIGHT CONDITIONS

Previous comparisons were conducted under LOS conditions. However, in practical deployments, CS will be more frequently used in NLOS environments. To evaluate performance under such conditions, the LOS results were compared with measurements taken under NLOS conditions using the same dataset spanning 1 to 10 meters. In the NLOS setup shown in Figure 4, an RF absorber was placed 50 centimeters from the initiator, ensuring the presence of multipath effects.

Figure 9 presents the results of this comparison. It can be observed that the differences between the three MUSIC variants are relatively minor, particularly in the lower error ranges, where the LOS setup only slightly outperforms the NLOS setup. However, as the error increases, the NLOS curve rises more steeply, suggesting that, while there is a measurable impact, it remains limited. These findings indicate that, with appropriate algorithm selection, low error ranging is still achievable under NLOS conditions, provided a stable BLE connection is maintained. Similar to the FFT results, one extreme outlier was removed from the NLOS MUSIC dataset to preserve the readability of the graph.

Higher distance ranges under NLOS conditions are analyzed in a manner consistent with the LOS scenario. As shown in Figure 10, the error increases beyond 10 meters, following a similar trend observed in LOS. This increase is most likely attributable to the same two contributing factors identified earlier.

As a supplementary check, shown in Figure 11, the slope-based algorithm was also evaluated under the same NLOS conditions. The results show a considerably higher average error, further confirming that MUSIC is significantly

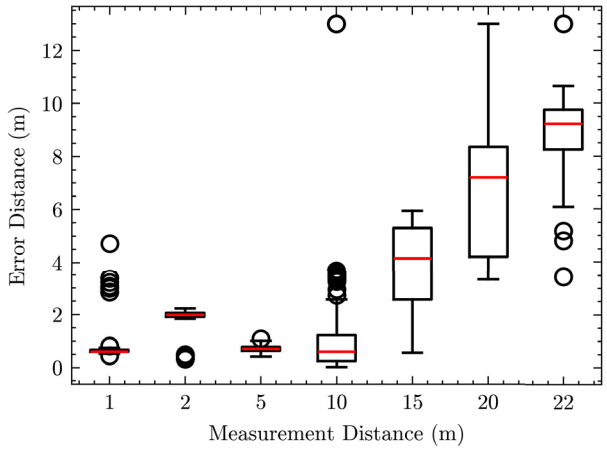

FIGURE 10. Distance estimation errors for MUSIC at various measurement distances, evaluated on an indoor NLOS dataset.

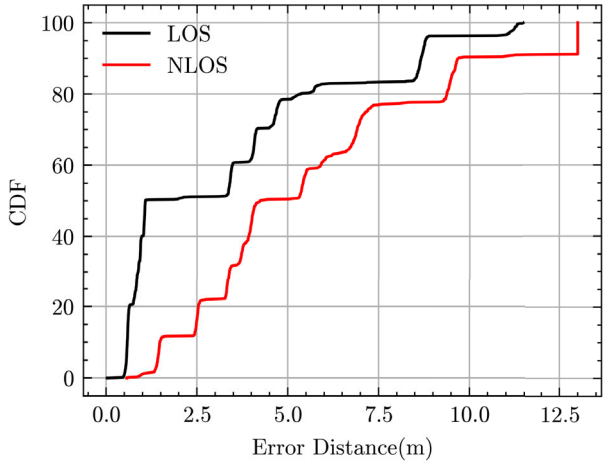

FIGURE 11. Distance errors for slope-based algorithm under both LOS and NLOS conditions, same indoor dataset as the MUSIC evaluation.

more robust than the slope-based approach in complex environments.

To reflect realistic deployment scenarios, we also evaluated NLOS conditions, as these are common in crowded environments such as public gatherings or events. In this secondary outdoor dataset, which included distances of up to 20 meters, an absorber was placed 50 cm in front of the initiator to simulate obstruction.

As expected, both the Slope and FFT methods exhibited performance degradation under NLOS. Up to the 70th percentile, their behavior remained comparable to indoor measurements. However, beyond this point, the outliers had a significantly greater impact than in LOS scenarios. Despite this, the slope-based method continued to perform best overall in the outdoor setting.

Interestingly, the MUSIC variations showed slight improved accuracy in the presence of the absorber. This unexpected result is visualized in Figure12, where error values are capped at 25 meters for clarity.

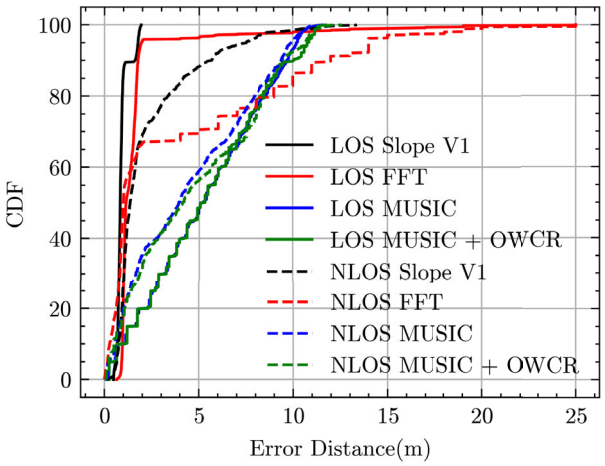

FIGURE 12. Outdoor distance errors for algorithms under both LOS and NLOS conditions.

C. EFFECT OF DEVICE ORIENTATION AND HEIGHT

Up to this point, all measurements were conducted with devices in fixed positions and antennas aligned directly toward each other. However, in real-world scenarios, device placement is often arbitrary, one device may be positioned higher than the other, and their orientations may vary both horizontally and vertically. To assess the impact of such variations, a series of measurements was performed with the devices placed 2 meters apart, systematically varying their relative orientations and heights, a set of orientations are shown in Figure 14.

1) HORIZONTAL ORIENTATION

Figure 13 illustrates the percentage of measurements falling below various error thresholds for multiple horizontal-laying orientation configurations, with the initiator's orientation represented on the vertical axis and the reflector's on the horizontal axis. Each configuration was evaluated using 100 measurements, resulting in a total of 2,500 samples. The MUSIC algorithm was employed for all evaluations.

The configuration in the top-left corner corresponds to the setup used in previous assessments and serves as a reference. Its results are consistent across all thresholds with those observed during earlier algorithm evaluations. Among the other configurations, notable differences emerge at the 50 cm and 60 cm thresholds. Specifically, configurations where the initiator faces away from the reflector tend to yield better accuracy, provided the reflector is not aligned parallel to the initiator, and in reverse as well. This observation is likely related to the radiation pattern of the onboard trace antenna, which, although intended to be omnidirectional, exhibits orientation-dependent gain variations that influence signal propagation and reflection.

Between the 60 cm and 75 cm thresholds, a substantial increase in successful measurements is observed, suggesting that while orientation does influence accuracy, the overall

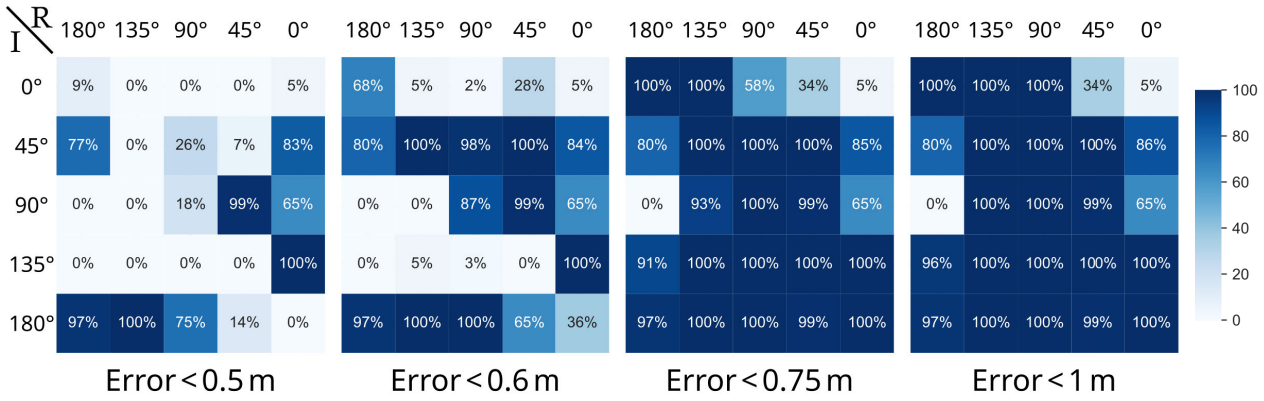

FIGURE 13. Impact of horizontal orientation on ranging accuracy, presented for each configuration across varying thresholds. Horizontal denote the orientation of the reflector, while vertical indicate the orientation of the initiator.

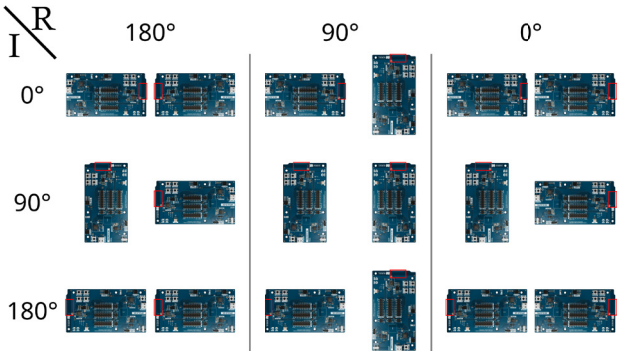

FIGURE 14. Top-down physical layout of a representative subset of tested orientations. The antenna is highlighted with a red rectangle.

variation between configurations remains relatively modest, even in a complex environment. However, certain orientations exhibit significantly reduced reliability, with some failing to produce a sufficient number of measurements below the 1-meter threshold. This indicates that while orientation may not always have a major impact, a small subset of configurations can be particularly volatile and should be carefully considered in system design to avoid performance degradation.

When the threshold is relaxed to 4 meters, not in the figure, nearly all configurations achieve 100% success, with the exception of the first row, third column, which reaches 99% due to a single extreme outlier.

2) IMPACT OF HEIGHT

As with the orientation analysis, an assessment was conducted to evaluate the impact of device height on ranging accuracy. Three different height levels were considered. The first, referred to as the mid-level height (approximately 80 cm above the ground), corresponds to the setup used in all previous experiments. The second, low-level, involved placing the devices directly on the ground. The third, high-level, positioned the devices on a stand to emulate ceiling-mounted deployment, while ensuring that they remained within the field of view of the MoCap system.

To capture a comprehensive dataset, multiple orientations were applied at each height, with the device orientation rotated in 90-degree increments. This resulted in a dataset comprising over 5,000 CS measurements. The devices were positioned with a separation of 2 meters, measured from a top-down perspective. However, due to elevation differences along the z-axis, the actual distance between devices exceeds this value. Nonetheless, the MoCap system captured the real distance. The results, categorized by varying error thresholds, are presented in Figure 15.

It was observed that the overall ranging error was higher compared to the orientation measurements. Consequently, slightly more forgiving error thresholds were selected: 50 cm, 75 cm, 1 meter, and 1.5 meters. The initiator-middle, reflector-middle configuration corresponds to the same dataset presented in Figure 13. In addition to the high-high and high-middle configurations, it consistently outperformed the others at lower error thresholds. However, even among the better-performing configurations, at least one orientation typically exhibited a significantly higher error. This suggests that the combination of orientation and height introduces amplifying effects on ranging accuracy. In particular, configurations such as high-low and low-high rarely achieved results below the 1-meter threshold. These configurations also involved the greatest actual distance between devices. Although it was observed above that the distance degrades the accuracy, the observed error escalation in these cases was steeper than that seen in previous experiments with longer horizontal distances alone. This indicates that factors beyond separation, such as vertical misalignment, may further impact ranging performance.

Once again, at the 4-meter error threshold, nearly all configurations achieved 100% success, with only a small number of outliers failing to meet the criterion.

3) MIXED ORIENTATION

In all previous orientation and height experiments, the devices were positioned horizontally. This final orientation evaluation

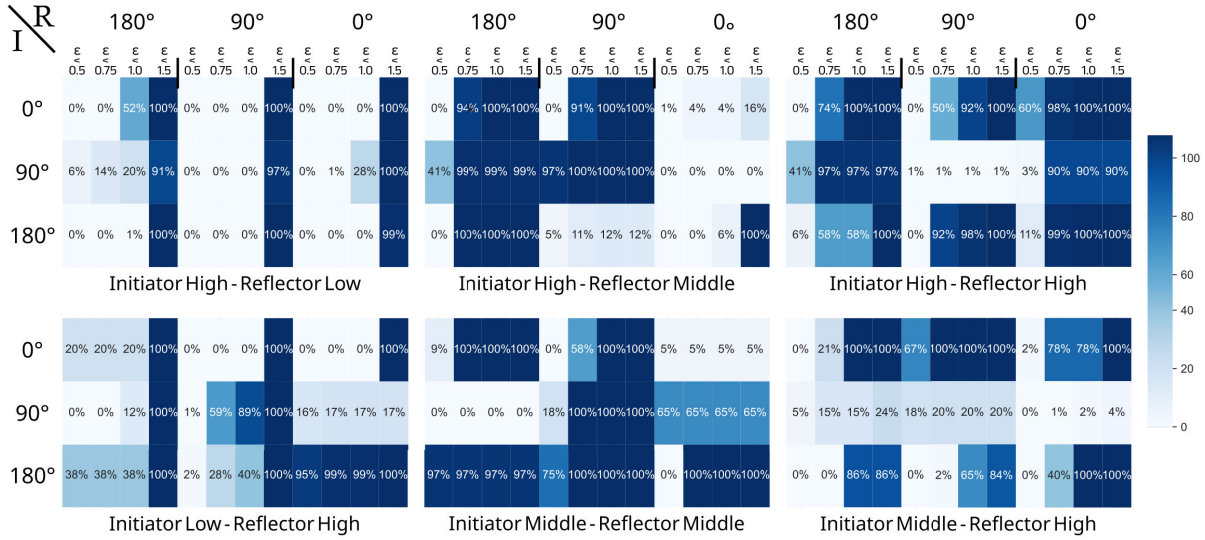

FIGURE 15. Impact of device height on ranging accuracy, shown across multiple orientation configurations and varying error thresholds. Horizontal represent the orientation of the reflector, while vertical indicate the orientation of the initiator.

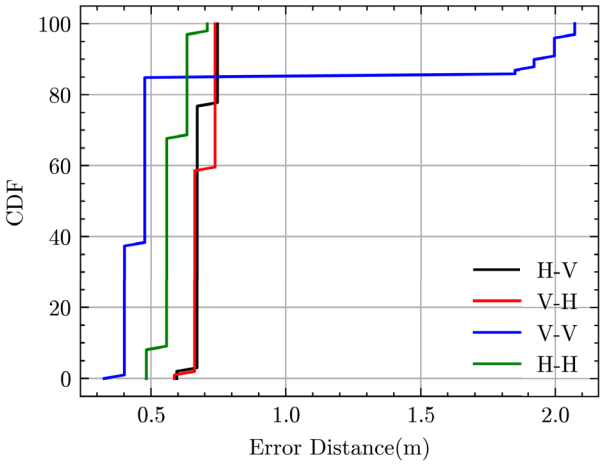

FIGURE 16. Distance estimation error for devices positioned horizontally (H) and vertically (V), evaluated using the MUSIC algorithm.

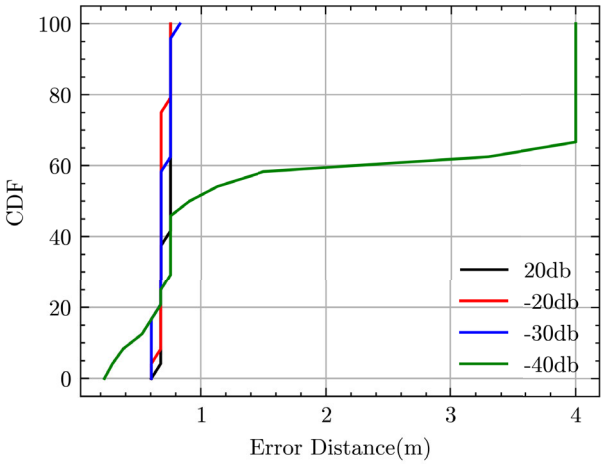

FIGURE 17. Distance error under higher power usage conditions.

investigates the impact of device orientation by comparing horizontal placement with vertical placement. As in earlier measurements, the devices were spaced 2 meters apart. Figure 16 presents the distance error for the four orientation combinations: vertical–vertical, horizontal–horizontal, and the two mixed configurations. The results indicate that orientation has a limited overall effect on accuracy. However, mixed configurations, where one device is vertical and the other horizontal, consistently yield the poorest performance. Fully vertical setups show a slight accuracy advantage over fully horizontal setups, though they also appear more susceptible to outliers.

D. INFLUENCE OF TRANSMISSION POWER AND PHY CONFIGURATION

1) TRANSMIT POWER

Ranging experiments were conducted on varying transmission power levels, starting from 20 dB, the maximum and default value used in all previous measurements, and incrementally decreasing down to the lowest supported hardware level of –127 dB, the time required to complete all measurements increased at progressively lower hierarchical levels. This was primarily due to persistent communication failures, which impeded coordination and led to significant delays in data collection. All measurements were performed at a fixed distance of 2 meters. Figure 17 presents the results for four selected power levels. As shown in the figure, the ranging accuracy remains stable for power levels exceeding –30 dB. However, once the transmission power drops below -40 dB, performance degrades significantly, with distance errors diverging sharply and many samples exceeding the 4-meter error threshold used for visualization.

Figure 18 further illustrates that all low-power configurations suffer from a comparable proportion of incorrect results. This degradation is primarily due to an increase in the

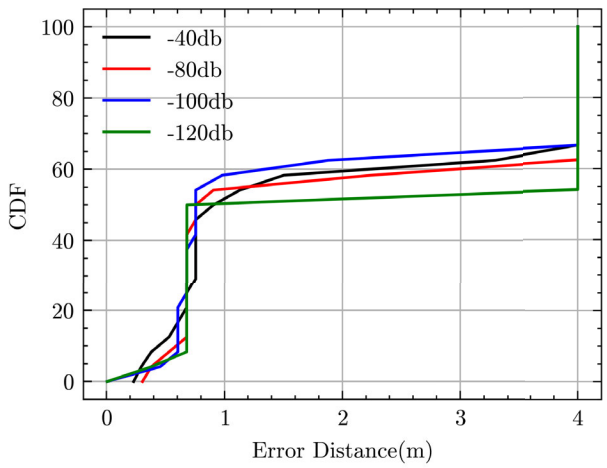

FIGURE 18. Distance error under lower power usage conditions.

number of signals that are classified as bad, as defined by the standard, which occurs more frequently at lower transmission powers. Although lower power is expected to reduce signal reliability over long distances, these results were obtained at only 2 meters of separation. This indicates that even in short range, low transmit power is insufficient for reliable ranging. Moreover, in NLOS scenarios, low-power signals often do not arrive entirely, making them unsuitable for dynamic or obstructed environments.

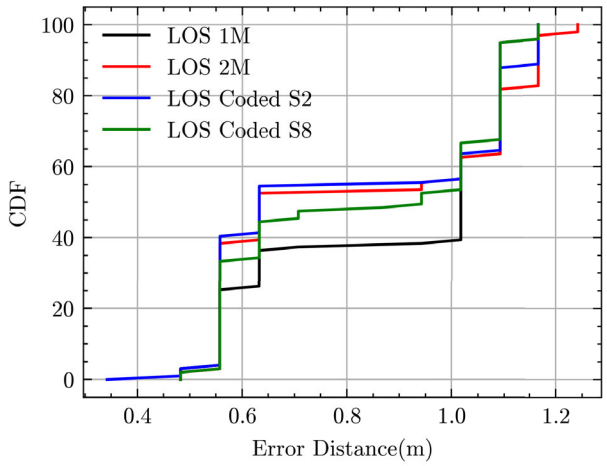

FIGURE 19. Distance error for different PHY settings.

2) IMPACT OF PHY

Bluetooth Low Energy supports multiple PHY data rates, each with its own advantages and limitations. This also applies to CS, where different PHY configurations may influence performance. However, as shown in Figure 19, the differences in distance estimation accuracy in the various PHY modes are minimal. These small variations are likely caused by environmental factors rather than the PHY settings themselves. Therefore, selecting a mode such as Coded S8 or 2M can be based on application-specific needs, such as range or data throughput, without significantly affecting the accuracy of the ranging results.

E. IMPACT OF CHANNEL AND STEP DOWNSAMPLING

In all previous measurements, the maximum number of steps per subevent was used, and the full Bluetooth spectrum of 72 channels was employed. However, in congested environments, where multiple devices may be performing ranging simultaneously or where numerous Bluetooth devices are active, this configuration can lead to increased signal collisions. To explore potential mitigation strategies, this section examines whether reducing the number of steps used for distance estimation and limiting the operation to subsets of the available spectrum can help alleviate the effects of interference and improve performance under such conditions.

TABLE 1. Average distance error and standard deviation across varying numbers of channels. For each channel count, multiple subsets of the spectrum were evaluated.

	20		30		40		50		72	
Type	μ	σ	μ	σ	μ	σ	μ	σ	μ	σ
Center	1.80	0.01	1.58	0.01	1.42	0.02	1.18	0.04	0.68	0.03
Left	1.89	0.02	1.47	0.05	1.34	0.07	1.05	0.01	/	
Right	1.81	0.01	1.65	0.01	1.43	0.01	1.22	0.08	/	
Spread	1.61	0.04	1.75	0.03	1.97	0.03	1.47	0.10	/	

1) CHANNEL SET SELECTION

Ranging measurements were conducted using different channel maps, all performed at a fixed distance of 2 meters, consistent with previous assessment experiments. Although the number of channels varied, 20 up to the full set of 72, the number of ranging steps remained constant across all configurations. As a result, configurations with fewer channels reused each channel more frequently, approximately 7–8 times for 20 channels, while in the full-spectrum case, each channel was used only 2–3 times.

Table 1 presents the average distance error and standard deviation for each configuration. The Center configuration refers to channel selections centered around channel 37. For the full 72-channel case, only the Center configuration is shown, as alternatives would be redundant. The Left and Right configurations consist of consecutive channels starting from channel 0 and starting at channel 77, respectively. The Spread configuration evenly divides the selected channels between the lower and upper ends of the spectrum.

The results indicate a clear relationship between the number of channels used and ranging accuracy: more channels generally lead to lower error. Among the different placement strategies, the Spread configuration shows slightly worse performance, suggesting that contiguous channel allocation is preferable. Minor differences were observed between the Left, Right, and Center configurations, but their impact on accuracy is relatively small.

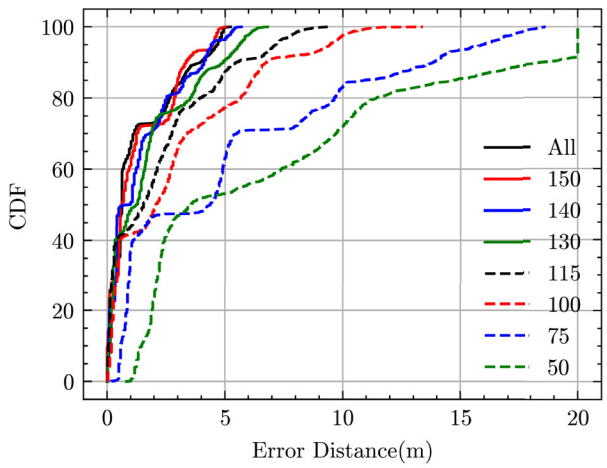

FIGURE 20. Distance estimation error as a function of the number of steps, evaluated using the same dataset employed for algorithm comparison.

2) NUMBER OF STEPS

One potential strategy for managing dense deployments of ranging devices is to reduce the number of steps used in the ranging process. To evaluate this, we downsampled the dataset previously used for algorithm comparison with various step counts. The original dataset contained 159 steps, and we tested reductions down to 50 steps, at which point not all channels are even represented. Although we also attempted a 25-step configuration, the MUSIC algorithm was unable to operate with such a limited number of In-phase and Quadrature (IQ) samples.

As shown in Figure 20, the performance with 50 steps is significantly degraded, with severe inaccuracies. For visualization purposes, the figure omits outliers beyond 20 meters; these only occurred in the 50-step configuration, where some estimates reached up to 40 meters.

In general, the results show minimal degradation between 159 and 140 steps. However, below this threshold, the accuracy deteriorates rapidly. In addition, fewer steps lead to increased sensitivity to outliers. This is due to reduced redundancy; at 140 steps, each channel is typically sampled twice, allowing poor measurements to be compensated for by others. With fewer steps, this redundancy is lost.

Although reducing the number of channels can mitigate this by increasing the number of samples per channel, it does not provide sufficient spectral diversity for algorithms to maintain precision, as previously shown. Therefore, combining step downsampling with reduced channel sets compounds the error, making such configurations unsuitable for accurate ranging.

Increasing the number of steps can improve accuracy, but it also leads to longer processing times. In applications where timing is more critical than precision, reducing the number of steps may be a practical consideration. However, under the current Bluetooth Channel Sounding standard, this trade-off has limited impact, as most of the time is spent transferring IQ samples over Bluetooth, which is still required. If future methods are developed to avoid or reduce this transfer process, the number of steps will have a more significant effect on timing and could then be optimized accordingly.

VI. DATASET AVAILABILITY

To facilitate reproducibility and further research, the collected IQ samples have been made publicly available on https://doi.org/10.5281/zenodo.17347695. Besides the measurement data, metadata and detailed information about the measurement environment are provided to enable additional insights. The data is stored in comma-separated value format, with each file corresponding to a specific distance used during Channel Sounding measurements. Each row in a file represents a single CS procedure and contains all associated steps, separated by commas.

Each step is structured as follows:

$$\texttt{initiator}_{\texttt{quality}};\ \texttt{reflector}_{\texttt{quality}};$$
$$\texttt{channel};\ \texttt{antenna};$$
$$\texttt{initiator}_{\texttt{i}};\ \texttt{initiator}_{\texttt{q}};$$
$$\texttt{reflector}_{\texttt{i}};\ \texttt{reflector}_{\texttt{q}}$$

The quality values are integers in the 2 bit range, computed according to the Bluetooth Core Specification 6.0 (Vol 6, Part H, Section 4.6), using the following equation:

$$IQ[dBm] = 20\log_{10}(abs(\frac{IQ[linear]}{2048}) + RPL[dBm]$$

The channel field indicates the frequency channel used, and antenna specifies the antenna index. For the single-antenna setup used in this study, this value is always 0. The I and Q components are signed 16-bit integers representing the raw signal samples.

In addition to the IQ data, ground truth and metadata are provided in accompanying spreadsheet files. These include the three-dimensional coordinates (x, y, z) of both devices at the time of measurement, as recorded by the motion capture system.

VII. CONCLUSION

The evaluations presented in this work demonstrate that the technology holds promise for applications such as keyless vehicle entry, where a certain margin of error, typically up to 3 meter, is acceptable. In such use cases, outliers can be mitigated through the proper use of RTT, and with a sufficiently high update rate, their impact can be effectively ignored.

However, the results also reveal that many of the evaluated factors, particularly orientation, height, power level, number of steps, and channel selection, significantly influence performance, despite the current MUSIC implementation being optimized for short-range scenarios. This effect is amplified in the case of outliers. As such, in its current form, a single-antenna setup is not sufficient for precise indoor

localization. Instead, the system behaves more like zone-based solutions, similar to those relying on RSSI.

Currently, the process of performing CS takes only a few milliseconds, which is acceptable for real-time localization. However, the transfer of IQ samples between the initiator and reflector over BLE can take up to 500 milliseconds, making the overall system response relatively slow. A potential solution would be to implement a synchronized backbone network, where IQ samples are transmitted to a central processing unit through a faster, shared infrastructure, allowing for more efficient and timely computation.

That said, these limitations do not preclude future utility. The algorithms tested in this study were relatively basic, and there is considerable potential for improvement. More advanced algorithms could be developed to account for the variability introduced by environmental and configuration factors. For example, the dataset collected in this work could serve as a foundation for machine learning-based approaches aimed at reducing sensitivity to such fluctuations.

Another promising direction is the integration of an Inertial Measurement Unit (IMU), which could help compensate for orientation-induced errors. Furthermore, the results show that the performance of the algorithms varies between scenarios, suggesting that intelligent algorithm fusion strategies could further enhance overall accuracy and robustness

In practical deployments, systems are often constrained by hardware limitations, particularly on the tag side. Tags typically have restricted space, limited computational resources, and tight power budgets, which constrain the number of antennas and the complexity of onboard processing. Consequently, careful consideration of device lifetime is essential, for instance, if the tag is only active during working hours, overnight charging can be a viable strategy to increase power. In contrast, anchor nodes are usually mains-powered and can accommodate more antennas and higher transmission power, offering less constraints and steer algorithmic design. Additionally, orientation is a critical factor that significantly affects performance but cannot be controlled in real-world scenarios. This highlights the need for further research into algorithms that are inherently robust to orientation variability, as current solutions often degrade under such conditions.

REFERENCES

[1] F. Zafari, A. Gkelias, and K. K. Leung, "A survey of indoor localization systems and technologies," *IEEE Commun. Surveys Tuts.*, vol. 21, no. 3, pp. 2568–2599, 3rd Quart., 2019.

[2] M. B. Kjærgaard, H. Blunck, T. Godsk, T. Toftkjær, D. L. Christensen, and K. Grønbæk, "Indoor positioning using GPS revisited," in *Proc. Pervasive Comput.*, 2010, pp. 38–56.

[3] T. Van Haute, E. De Poorter, P. Crombez, F. Lemic, V. Handziski, N. Wirström, A. Wolisz, T. Voigt, and I. Moerman, "Performance analysis of multiple indoor positioning systems in a healthcare environment," *Int. J. Health Geographics*, vol. 15, no. 1, p. 7, Feb. 2016, doi: 10.1186/s12942-016-0034-z.

[4] I. Silva, C. Pendão, and A. Moreira, "Real-world deployment of low-cost indoor positioning systems for industrial applications," *IEEE Sensors J.*, vol. 22, no. 6, pp. 5386–5397, Mar. 2022.

[5] A. De Angelis, M. Dionigi, A. Moschitta, R. Giglietti, and P. Carbone, "Characterization and modeling of an experimental UWB pulse-based distance measurement system," *IEEE Trans. Instrum. Meas.*, vol. 58, no. 5, pp. 1479–1486, May 2009.

[6] B. Alavi and K. Pahlavan, "Modeling of the TOA-based distance measurement error using UWB indoor radio measurements," *IEEE Commun. Lett.*, vol. 10, no. 4, pp. 275–277, Apr. 2006.

[7] Y. Liu and Y. Bao, "Real-time remote measurement of distance using ultra-wideband (UWB) sensors," *Autom. Construct.*, vol. 150, Jun. 2023, Art. no. 104849. [Online]. Available: https://www.sciencedirect.com/science/article/pii/S0926580523001097

[8] A. Makki, A. Siddig, M. Saad, and C. Bleakley, "Survey of WiFi positioning using time-based techniques," *Comput. Netw.*, vol. 88, pp. 218–233, Sep. 2015. [Online]. Available: https://www.sciencedirect.com/science/article/pii/S1389128615002169

[9] M. Uradziński, H. Guo, X. Liu, and M. Yu, "Advanced indoor positioning using ZigBee wireless technology," *Wireless Pers. Commun.*, vol. 97, no. 4, pp. 6509–6518, Dec. 2017, doi: 10.1007/s11277-017-4852-5.

[10] Bluetooth SIG. (2010). *Bluetooth Specification Version 4.0*. [Online]. Available: https://www.bluetooth.com/specifications/specs/core-specification-4-0/

[11] Y. Wang, X. Yang, Y. Zhao, Y. Liu, and L. Cuthbert, "Bluetooth positioning using RSSI and triangulation methods," in *Proc. IEEE 10th Consum. Commun. Netw. Conf. (CCNC)*, Jan. 2013, pp. 837–842.

[12] R. Ramirez, C.-Y. Huang, C.-A. Liao, P.-T. Lin, H.-W. Lin, and S.-H. Liang, "A practice of BLE RSSI measurement for indoor positioning," *Sensors*, vol. 21, no. 15, p. 5181, Jul. 2021. [Online]. Available: https://www.mdpi.com/1424-8220/21/15/5181

[13] G. Li, E. Geng, Z. Ye, Y. Xu, J. Lin, and Y. Pang, "Indoor positioning algorithm based on the improved RSSI distance model," *Sensors*, vol. 18, no. 9, p. 2820, Aug. 2018. [Online]. Available: https://www.mdpi.com/1424-8220/18/9/2820

[14] Bluetooth SIG. (2019). *Bluetooth Specification Version 5.1*. [Online]. Available: https://www.bluetooth.com/specifications/specs/core-specification-5-1/

[15] M. Woolley. (2019). *Bluetooth Direction Finding: A Technical Overview*. [Online]. Available: https://www.bluetooth.com/bluetooth-resources/bluetooth-direction-finding/

[16] G. Pau, F. Arena, Y. E. Gebremariam, and I. You, "Bluetooth 5.1: An analysis of direction finding capability for high-precision location services," *Sensors*, vol. 21, no. 11, p. 3589, May 2021. [Online]. Available: https://www.mdpi.com/1424-8220/21/11/3589

[17] Bluetooth SIG. (2024). *Bluetooth Specification Version 6*. [Online]. Available: https://www.bluetooth.com/specifications/specs/core-specification-6-0/

[18] M. Woolley. (2024). *Bluetooth® Channel Sounding Technical Overview*. [Online]. Available: https://www.bluetooth.com/channel-sounding-tech-overview/

[19] J.-Y. Jung, D. Kang, and C. Bae, "Distance estimation of smart device using Bluetooth," in *Proc. 8th Int. Conf. Syst. Netw. Commun.*, 2013, pp. 13–18.

[20] B. I. Ahmad, T. Ardeshiri, P. E. Langdon, S. Godsill, and T. Popham, "Modelling received signal strength from on-vehicle BLE beacons using skewed distributions: A preliminary study," in *Proc. 20th Int. Conf. Inf. Fusion (Fusion)*, Jan. 2017, pp. 1–7.

[21] J. Röbesaat, P. Zhang, M. Abdelaal, and O. Theel, "An improved BLE indoor localization with Kalman-based fusion: An experimental study," *Sensors*, vol. 17, no. 5, p. 951, Apr. 2017. [Online]. Available: https://www.mdpi.com/1424-8220/17/5/951

[22] P. Sambu and M. Won, "An experimental study on direction finding of Bluetooth 5.1: Indoor vs outdoor," in *Proc. IEEE Wireless Commun. Netw. Conf. (WCNC)*, Apr. 2022, pp. 1934–1939.

[23] M. Cominelli, P. Patras, and F. Gringoli, "Dead on arrival: An empirical study of the Bluetooth 5.1 positioning system," in *Proc. 13th Int. Workshop Wireless Netw. Testbeds, Experim. Eval. Characterization*, Oct. 2019, pp. 13–20, doi: 10.1145/3349623.3355475.

[24] M. Oshiro, S. Otaka, T. Kato, K. Nonin, M. Nishikawa, Y. Nito, H. Ishiwata, and H. Yoshida, "Sub-GHz phase-based ranging system: Implementation and evaluation," in *Proc. IEEE 91st Veh. Technol. Conf. (VTC-Spring)*, May 2020, pp. 1–7.

[25] M. Kotaru, K. Joshi, D. Bharadia, and S. Katti, "SpotFi: Decimeter level localization using WiFi," in *Proc. ACM Conf. Special Interest Group Data Commun.*, Aug. 2015, pp. 269–282, doi: 10.1145/2785956.2787487.

[26] S. Leitch, Q. Ahmed, W. Abbas, M. Hafeez, P. Lazaridis, P. Sureephong, and T. Alade, "On indoor localization using WiFi, BLE, UWB, and IMU technologies," *Sensors*, vol. 23, no. 20, p. 8598, Oct. 2023. [Online]. Available: https://www.mdpi.com/1424-8220/23/20/8598

[27] P. Corbalán and G. P. Picco, "Ultra-wideband concurrent ranging," *ACM Trans. Sensor Netw.*, vol. 16, no. 4, pp. 1–41, Sep. 2020, doi: 10.1145/3409477.

[28] P. Dabove, V. Di Pietra, M. Piras, A. A. Jabbar, and S. A. Kazim, "Indoor positioning using ultra-wide band (UWB) technologies: Positioning accuracies and sensors' performances," in *Proc. IEEE/ION Position, Location Navigat. Symp. (PLANS)*, Apr. 2018, pp. 175–184.

[29] F. Shan, H. Huo, J. Zeng, Z. Li, W. Wu, and J. Luo, "Ultra-wideband swarm ranging protocol for dynamic and dense networks," *IEEE/ACM Trans. Netw.*, vol. 30, no. 6, pp. 2834–2848, Dec. 2022.

[30] A. Santra, I. Kravets, N. Kotliar, and A. Pandey, "Enhancing Bluetooth channel sounding performance in complex indoor environments," *IEEE Sensors Lett.*, vol. 8, no. 10, pp. 1–4, Oct. 2024.

[31] A. Tsemko, A. Santra, O. Kapshii, and A. Pandey, "Data-driven processing using parametric neural network for improved Bluetooth channel sounding distance estimation," in *Proc. IEEE Int. Conf. Acoust., Speech Signal Process. (ICASSP)*, Apr. 2025, pp. 1–5.

[32] M. Nikodem, G. Trajnowicz, G. Salvatore de Blasio, and F. Alexis Quesada-Arencibia, "Experimental evaluation of multicarrier phase difference localization in Bluetooth low energy," *IEEE Sensors J.*, vol. 25, no. 1, pp. 1548–1560, Jan. 2025.

[33] D. Suresh, P. V. Joshi, P. Parandkar, A. Gambhir, and K. M. Sudharshan, "BLE channel sounding: Novel method for enhanced ranging accuracy in vehicle access," *IEEE Access*, vol. 13, pp. 67531–67547, 2025.

[34] J. P. Van Marter, A. G. Dabak, N. Al-Dhahir, and M. Torlak, "Support vector regression for Bluetooth ranging in multipath environments," *IEEE Internet Things J.*, vol. 10, no. 13, pp. 11533–11546, Jul. 2023.

[35] S. N. Shoudha, J. P. Van Marter, S. Helwa, A. G. Dabak, M. Torlak, and N. Al-Dhahir, "Reduced-complexity decimeter-level Bluetooth ranging in multipath environments," *IEEE Access*, vol. 10, pp. 38335–38350, 2022.

[36] Y. Chen, F. Yang, Y. Zhao, and X. Li, "High-precision ranging fusion using neural network for Bluetooth channel sounding," in *Proc. Int. Conf. Wireless Artif. Intell. Comput. Syst. Appl.*, 2025, pp. 131–142.

[37] P. Boer, J. Romme, J. Govers, and G. Dolmans, "Performance of high-accuracy phase-based ranging in multipath environments," in *Proc. IEEE 91st Veh. Technol. Conf. (VTC-Spring)*, Sep. 2020, pp. 1–5.

[38] P. Zand, J. Romme, J. Govers, F. Pasveer, and G. Dolmans, "A high-accuracy phase-based ranging solution with Bluetooth low energy (BLE)," in *Proc. IEEE Wireless Commun. Netw. Conf. (WCNC)*, Oct. 2019, pp. 1–8.

[39] J. R. Barr and M. McLaughlin, "Bluetooth-based ranging using channel sounding," U.S. Patent 10 708 970, Jan. 26, 2023. [Online]. Available: https://image-ppubs.uspto.gov/dirsearch-public/print/downloadPdf/10708970

[40] M. McLaughlin, J. R. Barr, and M. Woolley, "Bluetooth channel sounding with enhanced accuracy," U.S. Patent 11 743 852, Aug. 29, 2023. [Online]. Available: https://patents.google.com/patent/US11743852

[41] M. McLaughlin, J. R. Barr, and M. Woolley, "Bluetooth channel sounding for distance measurement," U.S. Patent 11 774 576, Oct. 3, 2023. [Online]. Available: https://patents.google.com/patent/US11774576

[42] Apple Inc., "Method and apparatus for wireless ranging using Bluetooth," E.P. Patent 3 839 562, Jul. 7, 2020. [Online]. Available: https://worldwide.espacenet.com/publicationDetails/biblio?CC=EP&NR=3839562

[43] H. Ólafsdóttir, A. Ranganathan, and S. Čapkun, "On the security of carrier phase-based ranging," in *Proc. Int. Conf. Cryptograph. Hardw. Embedded Syst.*, 2016, pp. 490–509.

[44] Bluetooth SIG. (2024). *Ranging Service 1.0*. [Online]. Available: https://www.bluetooth.com/specifications/specs/ranging-service-1-0/

[45] Nordic Semiconductor. (2025). *NRF54L15 DK*. Nordic Semiconductor. [Online]. Available: https://www.nordicsemi.com/Products/Development-hardware/nRF54L15-DK

[46] Nordic Semiconductor. (2025). *NRF Connect SDK*. [Online]. Available: https://github.com/nrfconnect/sdk-nrf

[47] Zephyr Project. (2025). *Zephyr*. [Online]. Available: https://github.com/zephyrproject-rtos/zephyr

[48] Nordic Semiconductor. (2025). *Bluetooth: Channel Sounding Initiator With Ranging Requestor*. [Online]. Available: https://github.com/nrfconnect/sdk-nrf/tree/v2.9-branch/samples/bluetooth/channel_sounding_ras_initiator

[49] IDLab. (2025). *Industrial IoT Lab*. [Online]. Available: https://idlab.ugent.be/resources/industrial-iot-lab

[50] A. Sheikh, J. Romme, J. Govers, A. Farsaei, and C. Bachmann, "Phase-based ranging in narrowband systems with missing/interfered tones," *IEEE Internet Things J.*, vol. 10, no. 17, pp. 15171–15185, Sep. 2023.

[51] F. Akbari, S. Shirvani Moghaddam, and V. Tabataba Vakili, "MUSIC and MVDR DOA estimation algorithms with higher resolution and accuracy," in *Proc. 5th Int. Symp. Telecommun.*, Dec. 2010, pp. 76–81.

JORG WIEME received the M.S. degree in computer science from Ghent University, Belgium, in 2021. He is currently pursuing the Ph.D. degree with IMEC, Ghent University. He joined the Internet Technology and Data Science Laboratory (IDLab) Research Group, IMEC, Ghent University. His research interests include multi-hop wireless networks, the Internet of Things (IoT), digital twin networks, le Audio, and distance ranging and localization.

RUBEN NIETVELT received the M.Sc. degree in applied engineering: electronics-ICT from the University of Antwerp, Belgium, in 2023. He is currently pursuing the Ph.D. degree with the University of Antwerp within the IDLab-IMEC Research Group. His research interests include integrated sensing and communication, as well as the use of wireless technologies for localization.

DRIES VAN LEEMPUT received the M.S. degree in electronics and ICT engineering technology, the M.S. degree in electronic engineering, and the Ph.D. degree in electronic engineering from Ghent University, in 2018, 2020, and 2024, respectively. During his doctoral studies, he was a member of the Technology and Data Science (IDLab) Research Group, IMEC, Ghent University and, focusing on multi-hop wireless sensor networks for industrial environments, the Internet of Things, energy harvesting, network and energy modeling, and MAC protocol design for critical wireless systems. In 2024, he joined Televic Healthcare as an Research and Development Engineer, where he currently develops next-generation nurse call products, emphasizing wireless communication, localization, and sensing technologies. He has contributed to several nationally and European-funded research projects.

MAARTEN WEYN received the Ph.D. degree in computer science on the topic of opportunistic seamless localization from the University of Antwerp, Antwerp, Belgium, in 2011. He is currently a Full Professor and the Vice-Rector of Research and Impact with the University of Antwerp. He teaches wireless communication systems and his research with IMEC-IDLab focuses on ultra-low power sensor communication, embedded systems, sub-1 GHz communication, sensor processing, and localisation. He Co-Founded spin-offs Aloxy, CrowdScan, IoSa, and AtSharp, contributed to 1OK and Viloc, and was a maker on the Canvas Program Team Scheire.

PIETER CROMBEZ (Member, IEEE) received the M.S. degree in electronic engineering from KU Leuven University, in 2005, and the Ph.D. degree in electronic engineering from KU Leuven University, in 2009, with his research on low power, reconfigurable transceivers for multistandard/multimode applications. He was a Research Assistant with the ESAT-MICAS Laboratory, KU Leuven University. He joined as the Research and Development Project Lead with Televic Healthcare in 2009, where he was responsible for the wireless research for next generation nurse call products. The main focus was on localization techniques that meet the harsh specifications for the healthcare market. Nowadays, holding the position of Research Lead, he is responsible for the long term research activities within Televic Healthcare with focus on wireless communication, localization and sensing. He has been involved in several national and European funded research projects, both as a participant and a project coordinator. He is a (co)author of several publications.

RAFAEL BERKVENS received the master's degree in applied engineering: electronics-ICT and the Ph.D. degree in indoor location information quantification from the University of Antwerp, Belgium, in 2012 and 2017, respectively. Currently, he is an Assistant Professor with IDLab-IMEC, Department of Electronic, Information and Communication Technology, Faculty of Applied Engineering, University of Antwerp. His research focuses on perception through ambient wireless communication, integrated sensing and communication, and intelligent transportation systems. He is a member of the IEEE Communication Society. He chairs the subject group of communication, teaches several networking courses, and coordinates part of the master's Project.

ELI DE POORTER received the M.S. degree in computer science engineering from Ghent University, Belgium, in 2006, and the Ph.D. degree from the Department of Information Technology, Ghent University, in 2011. He is currently a Professor with the IDLab Research Group, IMEC, Ghent University. His team performs research on wireless communication technologies, such as (indoor) localization solutions, the wireless IoT solutions, and machine learning for wireless systems. He performs both fundamental and applied research. For his fundamental research, he is currently the coordinator of several research projects (SBO, FWO, and GOA). For his applied research, he collaborates with industry partners to transfer research results to industrial applications, and to solve challenging industrial research problems. He has over 200 publications in international journals or in the proceedings of international conferences.

JEROEN HOEBEKE received the M.S. degree in computer science engineering from Ghent University, in 2002, and the Ph.D. degree in computer science engineering from Ghent University, in 2007, with his research on adaptive adhoc routing and virtual private ad-hoc networks. Currently, he is an Associate Professor with the Internet Technology and Data Science Laboratory, IMEC Ghent University. He is conducting and coordinating research on wireless (IoT) connectivity, embedded communication stacks, deterministic wireless communication, and wireless network management. He is the author or co-author of more than 200 publications in international journals or conference proceedings.